

# Chapter 6. Validation of LAI and $F_{PAR}$ products

M T Schaefer<sup>\*1, 2</sup>, E Farmer<sup>3</sup>, M Soto-Berelov<sup>3,4</sup>, W Woodgate<sup>3,4</sup>, S Jones<sup>3,4</sup>

<sup>1</sup> CSIRO Land and Water, Canberra, Australia

<sup>2</sup> Precision Agriculture Research Group, School of Science and Technology, University of New England, Armidale, Australia

<sup>3</sup> School of Mathematical and Geospatial Sciences, RMIT University, Melbourne, Australia

<sup>4</sup> Cooperative Research Centre for Spatial Information, Victoria, Australia

\*Corresponding author:

[Michael.schaefer@csiro.au](mailto:Michael.schaefer@csiro.au)

# Abstract

---

Leaf area index (LAI) and fraction of absorbed photosynthetically active radiation ( $f_{\text{APAR}}$ ) are two biophysical parameters that are closely related and often measured and validated in parallel in the field. LAI is typically defined as the total one-sided area of leaf tissues per unit of ground surface area. Utilizing this definition, LAI is a dimensionless unit which characterises the canopy of a given ecosystem (Breda, 2003). On the other hand,  $f_{\text{APAR}}$  is defined as the fraction of photosynthetically active radiation (PAR) in the 400-700 nm wavelengths that is absorbed by a canopy and it can include over-storey, understory and ground cover elements (Gower et al, 1999; Fensholt et al, 2004). This chapter provides a basic review of LAI and  $F_{\text{PAR}}$  product validation. After presenting a brief introduction of these concepts (LAI and  $f_{\text{APAR}}$ ), some of the major global LAI product validation programs are reviewed. This is followed by a discussion of different validation methods that can be used in the field and in situ sensors used to collect LAI and  $f_{\text{APAR}}$  measurements (e.g., Li-Cor LAI-2200, TRAC, AccuPar Ceptometer, Digital Hemispherical Photography (DHP) and the Plant Canopy Imager CI-110). The chapter finishes by presenting a methodology that illustrates MODIS collection 5 LAI validation efforts in Australian vegetated ecosystems.

## Key points

---

- Satellite derived LAI and fapar products can be validated across a range of scales, from local through to global.
- Validation can be achieved by comparing product values against reference data or by up-scaling observations gathered in the field using intermediate to large resolution imagery.
- Ground based measurements of LAI can be obtained directly when leaf area is physically measured or indirectly, by inferring LAI from other variables through observation (indirect non-contact techniques) or through the application of allometric equations (indirect contact techniques).
- Direct validation methods produce more accurate results given they avoid issues associated with foliage clumping and leaf angle distribution, however they are more labour intensive and time consuming than indirect methods. Accordingly, ground-based estimates of LAI are primarily acquired using indirect techniques.
- Allometric techniques establish a relationship between leaf area and another more easily obtainable variable such as DBH. However, allometric relationships tend to be site and time specific. The application of general allometric relationships as opposed to stand-specific ones can potentially result in moderate to large errors of estimated LAI values.
- Indirect, non-contact techniques to estimate LAI frequently rely on optical instruments that make use of radiative transfer theory to infer LAI from measurements of radiation transmission through the canopy. Optical instruments typically used to estimate LAI on the ground using indirect techniques include the LAI-2200 plant canopy analyser, the AccuPAR ceptometer, digital hemispherical photography (DHP), and the Tracing Radiation and Architecture of Canopies (TRAC) instrument.
- Indirect LAI estimates taken from indirect optical methods can be biased depending on the leaf inclination, canopy element clumping, and canopy cover characteristics, so they may require calibration via direct LAI measurements. Therefore, you cannot assume ground-based estimates are without error
- Given the variety of techniques and instruments available for measuring LAI, the most appropriate instrument is likely to be a function of the canopy structure and study area characteristics.

- LAI measurements using hemispherical photography and plant canopy analysers are best captured under completely diffuse lighting conditions such as dawn/dusk.
- LAI and fapar are associated metrics are frequently validated coincidentally.

## 6.1 Introduction

### 6.1.1 LAI

Leaf area index or LAI, typically defined as the total one-sided area of leaf tissues per unit of ground surface area (Breda, 2003)<sup>1</sup>, is a key biophysical parameter influencing vegetation photosynthesis, transpiration and energy balance at the land surface (Tian et al, 2002). LAI significantly influences the within and below canopy microclimate of a given vegetation stand controlling water interception, radiation transfer, water and carbon gas exchange (Breda, 2003). Consequently, LAI is an important driver in ecosystem productivity models, operating at local to global scales, and global models of climate, hydrology and biogeochemistry (Morisette et al, 2006) and is considered an Essential Climate Variable (ECV). There are several satellite derived LAI products (and a number of regional LAI mapping projects) that are available to the science community (Table 6.1).

**Table 6.1** Exemplar global LAI mapping projects.

Project	Agency	Sensor(s)	Website
<b>MODIS</b> (Moderate Resolution Imaging Spectrometer)	MODIS Land Team NASA	MODIS	<a href="http://modis-land.gsfc.nasa.gov">http://modis-land.gsfc.nasa.gov</a>
<b>POLDER</b> (Polarisation and directionality of the Earth's reflectance)	CESBIO/ CNES	POLDER-2	<a href="http://smc.cnes.fr/POLDER/">http://smc.cnes.fr/POLDER/</a>
<b>GLOBCARBON</b>	ESA	AVHRR VEGETATION POLDER MERIS	<a href="http://dup.esrin.esa.it/prjs/prjs43.php">http://dup.esrin.esa.it/prjs/prjs43.php</a>
<b>CYCLOPES</b> (Carbon Cycle in Land Observational Products from an Ensemble of Satellite)	European Union (FP5 project)	VEGETATION MERIS AATSR AVHRR	<a href="http://toyo.mediasfrance.org/?CYCLOPES-Project">http://toyo.mediasfrance.org/?CYCLOPES-Project</a>

<sup>1</sup> Utilizing this definition, LAI is a dimensionless unit which characterizes the canopy of a given ecosystem (Bréda, 2003). Multiple authors have identified issues regarding the application of this simplistic LAI definition (Hill et al, 2006; Zheng & Moskal, 2009, amongst others). Issues identified include the inability of this definition to accommodate needle-leaf canopies and those canopies characterized by vertical (erectophile) leaf angle distributions (Hill et al, 2006). This is particularly relevant to Australia, given the needle-leaf forms of frequently occurring species like Callitris, Casuarina and Acacia as well as the vertical leaf structure typical of Eucalyptus species (Hill et al, 2006). Such issues have resulted in a variability of LAI definition (see Zheng & Moskal, 2009 for a review). Consequently, there is a need to ensure the standardized definition, and appropriate documentation of all field based LAI measurements.

### 6.1.2 $f_{APAR}$

The parameter  $f_{APAR}$  is defined as the fraction of photosynthetically active radiation (PAR) in the 400-700 nm wavelength range that is absorbed by a canopy. However, this can include over-storey, understory and ground cover elements (Gower et al, 1999; Fensholt et al, 2004). It can be said then that  $f_{APAR}$  expresses the energy absorption capacity of a vegetation canopy (Fensholt et al, 2004) and is a key input to a number of primary productivity models based on simple efficiency considerations from local to global scales (Prince,1991).

$f_{APAR}$  is influenced by illumination conditions within a vegetation canopy. It varies with both sun position (solar zenith and azimuth angles) as well as atmospheric conditions (Weiss and Baret, 2011). Due to this, it is imperative that field validation of  $f_{APAR}$  is undertaken throughout the day under a variety of illumination conditions.

Similar to LAI, there are multiple satellite derived  $f_{APAR}$  products that are available to the science community including MODIS, POLDER, GLOBCARBON and CYCLOPES (Table 6.2). Such global products are supplemented by a number of regional  $f_{APAR}$  mapping projects that usually overlap/coincide with LAI mapping projects as the two products are closely related.

**Table 6.2** Exemplar global  $f_{APAR}$  mapping projects available to the community (adapted from Weiss et al, 2007).

Project	Agency	Sensor(s)	Website
NASA	MODIS	MODIS	<a href="http://modis-land.gsfc.nasa.gov">http://modis-land.gsfc.nasa.gov</a>
MGVI	ESA	MERIS	<a href="http://ntrs.nasa.gov/search.jsp?R=20010106090">http://ntrs.nasa.gov/search.jsp?R=20010106090</a>
POLDER	CNES	POLDER	<a href="http://smc.cnes.fr/POLDER/A_produits_scie.htm">http://smc.cnes.fr/POLDER/A_produits_scie.htm</a>
MERIS	ESA	MERIS	<a href="http://www.brockmann-consult.de/cms/web/beam/">http://www.brockmann-consult.de/cms/web/beam/</a>
CYCLOPES	European Union (FP5 project)	VGT	<a href="http://toyo.mediasfrance.org/?Projet-CYCLOPES,18">http://toyo.mediasfrance.org/?Projet-CYCLOPES,18</a>

## 6.2 LAI Validation

LAI products are validated by collecting LAI measurements across a range of scales, the largest of which consists of ground-based measurements. These can be compared directly against the coarse resolution LAI product values, as has been done to validate MODIS collection 4 LAI in Australia using hemispherical cameras to derive ground-based measurements of LAI (Hill et al., 2006; Sea et al., 2011). Validation can also be achieved by up-scaling observations to the coarse resolution satellite product. As will be described in the next section, ground based measurements can be obtained directly when leaf area is physically measured or indirectly, by inferring from other variables through observation or through the application of allometric equations as will be described below. Although direct methods are believed to be more accurate since they avoid issues associated with foliage clumping and leaf angle distribution, they are much more labour intensive and infeasible in many cases (Bréda, 2003; Jonckheere et al., 2004).

On a global scale, multiple agencies that are brought together under the CEOS WGCV - LPV subgroup have been working together to validate moderate resolution LAI products (Table 6.3). A thorough review of these projects is provided by Morisette *et al* (2006) with a summary given below:

- Boston University is responsible for the development of the NASA Earth Observing System (EOS) LAI products. Validation activities focus on the refinement and validation of LAI products and the algorithms driving the development of these products.

- The Validation of Land European Remote sensing Instruments (VALERI) program, primarily supported by CNES and INRA, focuses on the development of methodological approaches to support (a) the up-scaling of field measurements to generate high-spatial resolution maps of biophysical variables; and (b) the subsequent utilisation of these products to validate moderate resolution global products (Baret et al, 2005).
- The BigFoot program (1999 – 2003) grew out of projects that aimed to characterise Long Term Ecological Research (LTER) sites across the United States. The BigFoot project focuses on the validation of the MODIS derived LAI, land cover and net primary productivity land products (Cohen et al, 2006).
- The Canadian Centre for Remote Sensing (CCRS) produced LAI maps for Canada which have been validated across over 250 forest and shrubland dominated LAI plots. These 250 LAI plots were located in 10 study areas and aimed to sample a variety of Canadian forest types.
- The University of Alberta LAI studies focus on tropical forest regions. Satellite imagery, for both dry and moist tropical forest sites are used to study the relationship between field derived LAI and high-resolution satellite products.
- The United States Environmental Protection Authority (EPA) has conducted research to quantify error in the MODIS LAI product. The EPA has measured LAI (between 2001 and 2005) at six forested sites in North Carolina and Virginia in the United States of America.
- Research for the CARBOEUROPE project is conducted in Italy by the University of Milano-Bicocca. LAI measurements, sampled at 13 sites, have been collected with the aim of (a) developing localised relationships between canopy properties and carbon exchanges; and (b) validating moderate resolution, satellite derived LAI map products.
- The University of Helsinki, Finland, is working to develop more accurate LAI estimation methodologies within boreal conifer dominated regions.
- Penn State University's research focuses on the MODIS LAI products and their integration into crop models. The validation components of this research focus on the quantification of LAI uncertainty in products derived on corn, soybean and rice fields.

In addition, the CEOS WGCV - LPV has produced a global LAI product validation protocol (CEOS. 2014). This is a comprehensive review of current global LAI product validation methods and measurement techniques that also includes recommendations aimed at LAI product producers, LAI validation groups, the wider Science community, and CEOS. This is a valuable resource that includes definitions of key terms and good practice knowledge around validation procedures of satellite products. As the document evolves, it will be made available to the wider community through the CEOS WGCV LPV website (WWW1).

There is also an on-line validation web service (OLIVE) that has been designed to Quantify the performances of Earth observation land products (LAI, FAPAR, and FCOVER); use transparent and traceable methods following standards defined by the CEOS - LPV subgroup; provide open access of the results to the whole scientific community; and capitalize on the several initiatives undertaken within the community.

OLIVE (<http://calvalportal.ceos.org/olive>) is fully supported by the CEOS/LPV subgroup and allows users to reach Stages 2 and 3 of the validation process. In other words, it allows estimates of product accuracy over a significant set of locations and time through an inter-comparison exercise between existing products. Product uncertainty is quantified using reference in situ data over multiple locations representative of the Earth's surface. OLIVE is expected to eventually reach Stage 4 of the validation process following regular updates and an increasing participation of the scientific community.

Currently, OLIVE is running in beta mode, pending CEOS/LPV approval. Nevertheless, the scientific community can still access OLIVE to validate and inter-compare new products to existing ones. A validation exercise can be achieved in a private (results only accessible to user) or public mode (access to the whole OLIVE community).

**Table 6.3** Exemplar LAI validation campaigns, as outlined by Morisette et al, 2006.

Group	Field Instruments	Conversion of PAI to LAI	Understorey correction	Site extent	Sampling scheme	High resolution imagery	Transfer function	Accuracy of high-resolution LAI map	Sensor used
<b>Boston University</b>	LAI-2000	No	Yes	Various: from 5x5 km to 10x10 km	Two-stage	Landsat ETM+ (future: ASTER)	Parametric regression Fine-resolution MODIS algorithm	Derived from regression equations	MODIS
<b>VALERI</b>	LAI-2000 DHP	No	Yes	3x3 km	Two-stage	Landsat ETM+ SPOT HRVIR/HRG (future: ASTER)	Parametric regression Kriging	Cross validation and kriging variance	MODIS VEGETATION MERIS POLDER AVHRR
<b>BigFoot</b>	LAI-2000 Allometry Destructive harvest	No	No	5x5 km	Two-stage	Landsat ETM+ (future: ASTER)	Reduced major axis regression	Cross validation	MODIS
<b>CCRS</b>	LAI-2000 TRAC DHP	Species-based conversion factors	No	10x10km 150x150km	Two-stage	Landsat TM/ETM+	Parametric regression	Derived from regression equations	VEGETATION MODIS POLDER
<b>University of Alberta</b>	LAI-2000 DHP Litter traps	Using DHP from dry season and calibration from leaf litter and specific leaf area data	No	10x10km	Two-stage	Landsat ETM+ Hyperion IKONOS/Quickbird	Parametric & non-parametric regression, Bayesian network and Neural network	Calibration for dry forest	MODIS
<b>US EPA</b>	DHP TRAC	No	Yes (on two sites)	1x1km to 2x2km	Two-stage	Landsat ETM+ IKONOS	NA	NA	MODIS
<b>Italy</b>	LAI-2000 DHP Destructive harvest	No	Yes	From 250x250m to 1x1 km	Two-stage	Landsat ETM+ Hyper-spectral airborne	Parametric regression	Derived from regression equations	MODIS
<b>Finland</b>	LAI-2000	No	No	1x1 km (two sites) 3x3 km (two sites)	One-stage Two-stage	Landsat ETM+ SPOT HRVIR	Parametric regression	Derived from regression equations	MODIS
<b>Penn State</b>	LAI-2000 AccuPAR	No	No	1.6x1.6 km	One-stage	ASTER	In progress	NA	MODIS

### **6.2.1 Direct field measurement of LAI**

Direct measurements of LAI are based on the measurement of leaf area where leaves are collected via techniques like harvesting or litter collection. Area harvesting techniques require the periodic, destructive sampling of all vegetation within the sample plot during the growing season (Gower *et al*, 1999). Such destructive harvesting of a sample plot is based on the up-scaling of measurements to the vegetation patch or stand and, as a consequence, assumes lateral homogeneity. In other words, it is assumed that the plot is representative of the stand (Jonckheere *et al*, 2004).

In deciduous stands, an additional measure of leaf area can be estimated from litter traps. The advantage of this approach is that it is non-destructive. Litter traps are based on the collection of leaf litter from a specified ground area. Multiple collections are made over the leaf fall period to prevent the loss of leaf material due to decomposition processes (Breda, 2003). LAI is estimated from the accumulated leaf area over all leaf fall collections and thus represents an integrated measure of LAI over the measurement time period. However, authors note that the litter trap collection cannot provide estimates of LAI (a) at a single moment in the growing season nor (b) within temporal or vertical profiles (Jonckheere *et al*, 2004). At the same time, there is no consensus on the location or sample design of litter traps (Jonckheere *et al*, 2004), therefore extensive experimental documentation is essential.

Subsequent to leaf collection via harvesting or litter collection, leaf area is calculated within planimetric or gravimetric approaches. The first are based on a contour assessment, and subsequent area calculation, of the leaf in a horizontal plane (Jonckheere *et al*, 2004). Various planimeters are available for this purpose. Conversely, gravimetric methods correlate the dry weight of the leaves to leaf area. Such measurements are typically applied to a sub-sample of leaves in order to develop a relationship between area and dry mass, that is, the specific leaf area (SLA,  $\text{cm}^2 \text{g}^{-1}$ ). This leaf area (SLA) to mass ratio is variable as a function of both species and site characteristics (Breda, 2003).

The harvesting of all vegetation, within a predefined sample plot, is widely utilised when measuring the leaf mass of crop or pasture areas (Breda, 2003). However, the exhaustive, potentially time consuming (Jonckheere *et al*, 2004) and destructive characteristics of this technique limit its applicability to forest canopies (Breda, 2003). Consequently, allometric measurements are more frequently used within forested canopies.

### **6.2.2 Indirect field measurement of LAI**

Indirect techniques typically infer leaf area from observations of another variable. Such techniques are generally less destructive and time consuming than the previously outlined direct approaches. Jonckheere *et al* (2004) classify indirect, ground-based LAI measurement techniques into two categories (a) indirect contact LAI measurements; and (b) indirect non-contact LAI measurements. Such a categorisation will be utilised in the following discussion.

#### ***Indirect contact LAI measurements***

Allometric techniques establish a relationship between leaf area and the dimension of woody elements within a tree. For example, established allometric equations can relate leaf area (determined via destructive harvest), to the sapwood area at tree breast height or the crown base (Jonckheere *et al*, 2004). Such equations are based on the assumption that leaf area is in balance to the amount of connective tissue

within the tree (Breda, 2003). Proposed modifications to this relationship include the inclusion of sapwood permeability (Jonckheere *et al*, 2004). The complexity of quantifying sapwood diameter and permeability (Breda, 2003; Jonckheere *et al*, 2004) has led to the development of multiple allometric equations which are not reliant upon this measure. Frequently utilised woody measurements include stem diameter, stem density, tree height and crown base height (Jonckheere *et al*, 2004; Jupp *et al*, 2008).

Allometric relationships have been demonstrated to be site and time specific (Breda, 2003; Jonckheere *et al*, 2004). Equally, sapwood area/leaf area relationships have been shown to be dependent upon tree size, season, nutrient availability, soil water availability, local climate and canopy structure (Gower *et al*, 1999; Jonckheere *et al*, 2004). Such abiotic and biotic factors can result in moderate to large errors in LAI derivation for a stand when general allometric relations, as opposed to stand-specific ones, are implemented (Gower *et al*, 1999).

There are additional techniques capable of providing indirect measures of leaf area. One of these is the line-intercept method, which involves conducting a vertical transect through the canopy under known elevation and azimuth angles (Jonckheere *et al*, 2004).

### ***Indirect non-contact LAI measurements***

Indirect, non-contact techniques frequently rely on optical instruments that make use of radiative transfer theory to infer LAI from measurements of radiation transmission through the canopy (Breda, 2003; Jonckheere *et al*, 2004). Such techniques are advantageous in that they are non-destructive. Indirect measurements do not, typically, estimate LAI given they usually consider all canopy elements (woody and non-woody) within their field-of-view; as opposed to measuring only the green leaf area. Consequently, the terms Plant Area Index (PAI) or Surface Area Index (SAI) are commonly utilised when estimating LAI via indirect measurement techniques (Breda, 2003).

Multiple optical instruments indirectly estimate LAI from measurements of the canopy gap fraction, where canopy gap fraction is derived from measurements of radiation transmission through the canopy. LAI is calculated by inversion of the exponential expression of the gap fraction. Gap fraction or gap probability '*P<sub>gap</sub>*' may be defined as the proportion of canopy gaps visible in a given viewing direction. LAI is a function of several structural attributes that affect the extinction of light within plant canopies and consequently the remote sensing signal, namely the; (i) proportion and density of leaf and non-leaf components (these attributes combine to give the metric PAI) (ii) canopy element angle distribution, and (iii) degree of canopy element clumping. Each of these structural attributes can vary substantially with viewing angle, scale, and environment, even amongst stands of the same species. The physical formulation of LAI and canopy gaps is based on the Beer-Lambert law, relating the attenuation of light to the properties of the material through which the light is travelling (Lambert, 1760). Nilson (1971) demonstrated how the directional gap probability *P<sub>gap</sub>*( $\Phi$ ,  $\theta$ ) ( $\Phi$  = azimuth angle,  $\theta$  = zenith angle) of an incident beam of radiation will pass through a clumped canopy to reach a given point inside or below the canopy using the modified Beer-lambert law of light extinction. Chen *et al*. (1996) modified Nilson's formulation to account for the proportion of woody elements ' $\alpha$ ', which was subsequently modified by Woodgate *et al*. (in review) to account for the angular nature of woody elements:

$$LAI = \frac{-\log P_{gap} \tau(\theta) \cos(\theta) (1-\alpha)}{G_T(\theta) \Omega_T(\theta)} \quad (\text{equation 6.1})$$

Where *P<sub>gap</sub>*( $\theta$ ) is the gap probability of all canopy elements (i.e. leaf and wood), *G<sub>T</sub>*( $\theta$ ) is the combined projection coefficient of wood and leaf elements,  $\Omega_T(\theta)$  is the total clumping factor of all canopy elements, and  $\alpha$  is the woody-to-total-area ratio.  $\cos(\theta)$  is the correction for path length through the canopy, which increases with



higher zenith angles.  $\alpha$  relates the woody projection function 'G<sub>w</sub>' and leaf projection function 'G<sub>L</sub>' coefficients to the total element projection function 'G<sub>T</sub>' by:

$$G_T(\theta) = (1 - \alpha)G_L(\theta) + \alpha.G_W(\theta) \quad (\text{equation 6.2})$$

**Eqn. 6.1** assumes a random orientation in azimuth angle for both woody and leaf components. In many cases this would be a valid assumption for woody components since; (i) for typically cylindrical vertical tree stems, a large proportion of the woody surface area is in the stem, and (ii) most stem and branch components in the trunk are circular in nature, and typically spread radially throughout the branching orders, thus leading to a more equal probability of occurrence in all azimuth directions. Therefore, the projected area of leaf and woody canopy elements becomes a function of only zenith view angle when this assumption is satisfied.

Most plant canopies are typically clumped to some degree, which is scale dependent. Chen *et al* (1997) proposed that without correction for non-random canopy element distribution, the result is the effective LAI (LAI<sub>e</sub>) or effective PAI (PAI<sub>e</sub>), depending on whether a correction for  $\alpha$  was made or not.  $\Omega(\theta) = 1$  occurs when the spatial distribution of elements are random,  $\Omega(\theta) < 1$  implies a clumped or aggregated canopy, and  $\Omega(\theta) > 1$  implies a regularly distributed canopy, where less gaps are visible than a theoretically random canopy with the same PAI and G( $\theta$ ). The authors state that with multiple angle measurements of  $P_{gap}(\theta)$  and G( $\theta$ ), the PAI<sub>e</sub> can be calculated simultaneously. Additionally, single narrow angular gap fraction of approximating single view zenith angles has also been used to estimate PAI<sub>e</sub> (Neumann *et al*, 1989; Leblanc & Chen, 2001). However, without knowledge of the spatial distribution of leaves within the canopy ( $\Omega$ ) only the product of  $\Omega$  and PAI can be calculated. Chen *et al* (1997) utilise PAI<sub>e</sub> for the derivation of LAI in clumped canopy comprising both leaf and wood elements following the equation:

$$LAI = (1 - \alpha) \frac{PAI_e}{\Omega} LAI = (1 - \alpha) \frac{LAI_e}{\Omega} \quad (\text{equation 6.3})$$

Where  $\alpha$  is the woody-to-total plant area ratio and  $\Omega$  is a parameter determined by the spatial distribution of leaves within the canopy. PAI<sub>e</sub> is typically measured at the ground surface and includes the contribution of dead leaves, woody branches and trunks. As such, measurements represent SAI or PAI. A factor (1 -  $\alpha$ ) is used to remove the contribution of non-leafy surfaces from the PAI<sub>e</sub> measurement (Chen *et al*, 1997). Note that PAI<sub>e</sub> in Eqn. 6.3 is equivalent to  $-\log(P_{gap_T}(\theta)).\cos(\theta) / G(\theta)$ . Also note that  $(1 - \alpha).PAI_e = LAI_e$ .

An important element of equation (6.3) is the fact that PAI<sub>e</sub> can be calculated without prior knowledge of the foliage angle distribution if the gap fraction is estimated at multiple zenith angles (Chen *et al*, 1997) using a modified version of Miller's formula Miller (1967):

$$PAI_e = 2 \int_0^{\pi/2} -\ln(P_{gap}(\theta_v)) \cos \theta_v \sin \theta_v d\theta_v \quad (\text{equation 6.4})$$

$$W_i = d\theta_i \cdot \sin \theta_i / \sum_{i=1}^{i=n} d\theta_i \cdot \sin \theta_i \quad (\text{equation 6.5})$$

Where  $P_{gap}$  denotes the gap fraction and  $\vartheta_v$  denotes the view zenith angle.  $P_{gap}(\vartheta_v)$  is averaged per zenith ring, where each ring has a ring centre angle  $\vartheta_i$  and angular width  $d\vartheta_i$ .  $i$  denotes the zenith ring number,  $n$  is the number of zenith rings. Utilising zenith rings allows discretisation of the instrument field-of-view into smaller zenith segments in order to compute multiple  $P_{gap}$  estimates for input into Eqn. 6.4. The sum of  $W_i$ , the zenith ring weighting function (Eqn. 6.5), for all  $n$  is equal to unity. LAI<sub>e</sub> can be calculated from Eqn. 6.4 using angular  $P_{gap}$  measurements. The correct method for estimating LAI<sub>e</sub> from multiple measurement locations, such as a plot, is to first average the angular  $P_{gap}$  over all measurement locations, and then apply Eqn. 6.4 (Ryu *et al*, 2010). This ensures no correction for non-random distribution of clumping at scales larger than the measurement

location, caused by the potential logarithmic averaging of LAI<sub>e</sub> that may occur at multiple measurement locations (Kucharik *et al*, 1997; Ryu *et al*, 2010).

### The extinction coefficient $k$

Monsi and Saeki (1965) provided a theoretical relationship of light extinction coefficient ' $k$ ' to LAI in a plant community based on a form of the Beer-Lambert law (Lambert, 1970). Their model provided a basis for many subsequent studies, both experimental and theoretical, and continues to be used to this day:

$$\frac{I}{I_0} = e^{-k.LAI} \quad (\text{equation 6.6})$$

Where  $I$  is the light intensity under the LAI layer,  $I_0$  is the light intensity above the LAI layer, and  $k$  is the extinction coefficient. The ratio  $I:I_0$  is equivalent to light transmittance or  $P_{gap}$  at the point of measurement.

$k$  is essentially a function of leaf clumping, leaf angle projection and view zenith angle when the assumption of a horizontally continuous canopy with no woody elements is met. However, this model has been further expanded to account for the impact of woody components on the element projection function and clumping (Woodgate *et al.*, in review). A parameterisation of  $k$  is as follows for a canopy with foliage and woody elements:

$$k(\theta) = G_T(\theta)\Omega_T(\theta)/\cos(\theta)(1 - \alpha) \quad (\text{equation 6.7})$$

Eqn. 6.7 can be modified for the case of an individual tree encompassed by a geometric volume or object, such as a cylinder, as follows:

$$k(\theta) = G_T(\theta)\Omega_T(\theta)/l_{ave}(\theta)(1 - \alpha) \quad (\text{equation 6.8})$$

Where  $l_{ave}$  is the average path length through the geometric volume encompassing the tree. Eqn 6.7 incorporates clumping at all scales, e.g. between crown and within crown. Eqn. 6.8 incorporates within-crown clumping only for crowns encased in a geometric shape.

We know that  $k$  is a function of  $G$  and  $\Omega$ , which are both independently measureable quantities. Therefore, Woodgate *et al.* (in review) recommended splitting  $k$  into its measureable sub-components so that assumptions and its derivation are explicit. This makes  $k$  more comparable for other studies, and also enables uncertainty estimates to be placed on the metric. A general outline of independent methods to estimate each parameter of  $k$  (Eqn. 6.7, 6.8) and LAI (Eqn. 6.1) are presented.

### Canopy gap fraction ' $P_{gap}$ '

Multiple canopy analysers, based on the above principles, measure the transmittance of radiation through the canopy. These instruments include, but are not limited to, the (a) SunSCAN (Delta-T Device Ltd, Cambridge, UK); (b) AccuPAR ceptometer (Decagon Devices, Pullman, USA); (c) LAI-2200 plant canopy analyser (Li-Cor Inc., Lincoln, Nebraska, USA); (d) DEMON instrument (CSIRO); and (e) Terrestrial Laser Scanning (TLS) (Table 6.4). Such devices differ in their measurement characteristics. For example, the SunSCAN and AccuPAR devices measure the incident and transmitted photosynthetically active radiation (PAR) while the LAI-2200 measures the canopy gap fraction from multiple zenith angles (Table 6.4). Transmittance is analogous to  $P_{gap}$ . When optimal instrument lighting conditions are met, the difference between transmittance and  $P_{gap}$  are negligible; such as uniform diffuse lighting with a uniform sky background or conversely direct lighting conditions (Table 6.4). In both instances, the optimal lighting conditions are stable; and the foliage is assumed to be black with no multiple scattering of radiation, which is more prevalent in direct sunlit conditions.

**Table 6.4** LAI/PAI canopy analysers (adapted from Breda, 2003). Ordered from left to right in popularity for frequency of use.

	DHP	LAI-2200	AccuPAR	SunScan	TRAC	TLS	DEMON
Company	Many specialised and non-specialised	LI-COR, Lincoln, Nebraska, USA	Decagon Devices, Pullman, ISA	Delta-T Devices Ltd, Cambridge, UK	3 <sup>rd</sup> Wave Engineering, Ontario, Canada	Many commercial and some non-commercial	CSIRO
Principle	Gap fraction for each zenith angle acquired simultaneously	Gap fraction for each zenith angle acquired simultaneously	Gap fraction or sunflecks	Gap fraction or sunflecks	Gap size distribution from transects at one zenith angle	Gap fraction for each azimuth and zenith angle with range to target recorded	Gap fraction zenith angles from the sun at different angles to the vertical
Waveband	400-700nm typical	320-490 nm	400-700 nm	400-700 nm	400-700nm	900nm, 1550 nm typical	430 nm
Illumination conditions	Uniform overcast sky or clear sky at sunset or sunrise	Uniform overcast sky or clear sky at sunset or sunrise	Wide range of daylight condition. Best in bright sunlight	Wide range of daylight condition. Best in bright sunlight	Direct sunlight conditions on a clear day	Day or night	Clear bright day from early morning until noon
Leaf separation	Yes	No	No	No	No	Yes	No

### Correction for the proportion of woody material ' $\alpha$ '

Frequently, it is hard to distinguish foliage from woody elements such as branches and trunks using indirect methods such as DHP and TLS. Because of this, PAI is derived instead of LAI. An area under current investigation is the separation of woody from non-woody elements from indirect techniques. The separation of leaf and wood can be used to estimate the proportion of woody to total plant area ' $\alpha$ '. Techniques used to estimate alpha include: destructive harvesting (Gower *et al*, 1999), classification of woody and non-woody canopy elements with RGB DHP (Sea *et al.*, 2011) or near-infrared cameras (Fig. 6.2, Kucharik *et al*, 1998), and Terrestrial Laser Scanning (Béland *et al*, 2014; Danson *et al*, 2014).

### Foliage and Wood angle distribution and projection functions ' $G_L$ ' and ' $G_W$ '

The leaf and non-leaf (wood) element angle distributions are used to characterise the projected leaf area ( $G_L$ ) and wood area ( $G_W$ ) as a function of viewing angle. A number of direct and indirect techniques to measure leaf inclination angles exist (e.g. directly with a plumb-bob and protractor or indirectly from levelled photos, Ryu *et al*, 2010). Replicating leaf angle measurement techniques on woody components may be challenging. However, due to recent advances in semi-automated tree reconstruction methodologies (Côté *et al*, 2009; Raunonen *et al*, 2013), 3D computer reconstruction models can be efficiently queried to determine the element distribution functions and subsequently to derive  $G_W$  and  $G_L$  precisely. Conversely,  $LAI_e$  and  $PAI_e$  can also be estimated without prior knowledge of the foliage and wood angle distribution at the narrow zenith angle range centered on  $\theta \approx 57.3$  degrees, where foliage angle projection functions (Wilson 1963; de Wit, 1965) and wood angle projection functions (Woodgate *et al*, in review, RSE) have been shown to converge. Therefore, both  $G_L$  and  $G_W$  may not

need to be measured in the field if inverting over a narrow gap fraction range ( $\pm \approx 2.5$  degrees) centered on the 57.3 degree zenith angle.



**Figure 6.2** Infrared camera (Canon EOS 450D with the Sigma 8mm EX fisheye lens) used in the Robson Creek rainforest in Far North Queensland. The use of infrared cameras can assist distinguishing woody versus non-woody elements in a canopy.

### Canopy element clumping ‘ $\Omega$ ’

A number of instruments employ clumping retrieval methodologies, which are typically based on logarithmic averaging of  $P_{gap}$  or gap size distribution information (Leblanc *et al*, 2014). DHP can be utilised to estimate various clumping retrieval methods such as the: ‘LX’ (Lang and Xiang, 1986), ‘CCL’ (Chen & Cihlar, 1995) later modified by Leblanc (2002a), ‘CLX’ (Leblanc *et al*, 2005), and ‘CMN’ methods (Pisek *et al*, 2011), all following nomenclature by Leblanc *et al*. (2014). The LAI-2000/2200 instruments employ the LX method, and the TRAC instrument employs the CCL method. Other methodologies such as Jupp *et al*. (2008), which was developed for TLS, may subsume clumping values into their final PAI estimate. An exemplar procedure for estimating clumping from DHP is provided in **section 6.4.1**.

Some typical indirect non-contact instruments that are used to estimate LAI in the field are outlined below.

- **Digital Hemispherical photography (DHP)**

Hemispherical photography is a technique for quantifying plant canopies via photographs captured through a hemispherical or fisheye lens (Figure 6.1). Such photographs can be captured from beneath the canopy, looking upwards, (orientated towards zenith) or above the canopy looking downwards (Jonckheere *et al*, 2004). Hemispherical photographs produce a projection of the hemisphere onto a plane. The nature of this projection is a function of the lens utilised. However, the simplest and most common hemispherical lens geometry is the polar or equi-angular projection (Jonckheere *et al*, 2004).

With increases in the availability of digital cameras and image processing software digital hemispherical photography (DHP) is increasingly being used in addition to or as a replacement for other canopy analysers (Breda, 2003). DHP represents a rapid, low-cost and non-destructive methodology for the (a) estimation of LAI (Jupp *et al*, 2008); and (b) creation of a permanent canopy structure records. Such records include species, site and age-related differences in canopy architecture (Jonckheere *et al*, 2004).

Multiple software packages are available to support the derivation of canopy gap fraction, and its subsequent conversion to LAI, from DHP. For example, CAN-EYE was developed as part of VALERI (Baret *et al*, 2005). This dedicated image processing software is required to separate sky (or soil for downward looking) and plant canopy elements in the photographs, derive the canopy gap and subsequently convert the gap fraction to LAI. Determination of an appropriate threshold to separate these elements is fundamental to the accurate estimation of canopy gap fraction and LAI via these techniques (White *et al*, 2000).

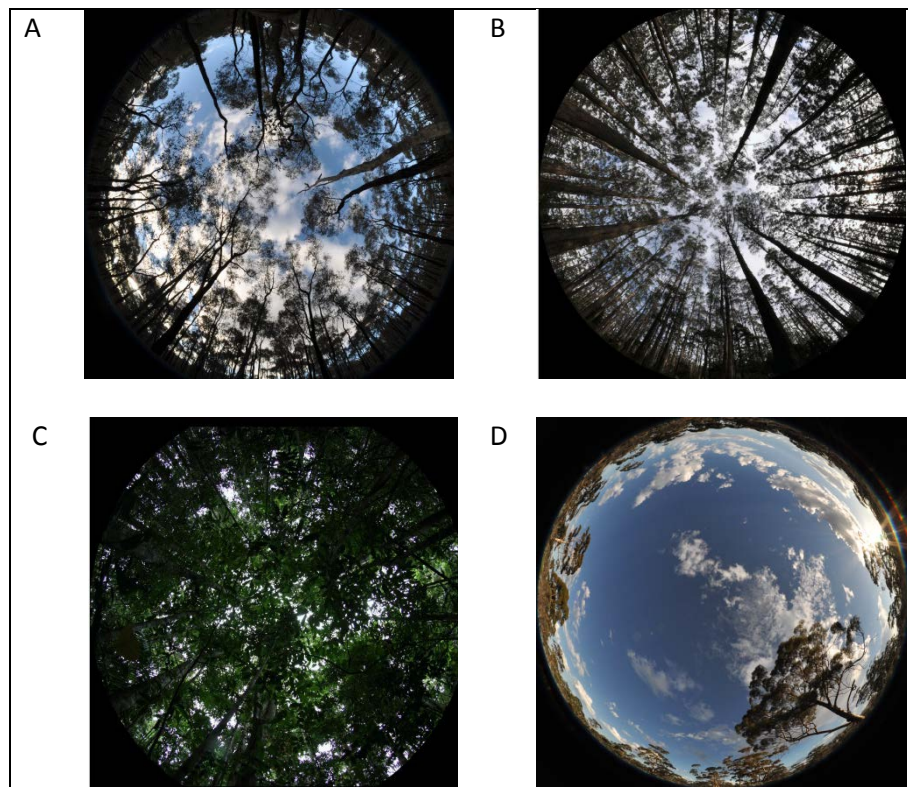


**Figure 6.1** Examples of DHP in various forest environments: A) Dry sclerophyll forest near Nagambie, Victoria<sup>^</sup>; B) Mountain Ash forest near Watts Creek, Victoria<sup>^</sup>; C) Wet tropics rainforest in Robson Creek, Far North Queensland (EOS 50D with a Sigma 8mm EX fisheye lens); D) Great western woodlands near Kalgoorlie, Western Australia<sup>^</sup>. <sup>^</sup> denotes the Nikon D90 with a Sigma EX 4.5mm circular fisheye lens

Hemispherical cameras also have the advantage of (a) enabling efficient estimates of canopy clumping through various gap size inversion techniques (Leblanc *et al*, 2014); (b) being applicable in low and high canopies (by taking downward and upward looking photographs); (c) less sensitive to variable illumination conditions; and (d) are a permanent record of canopy structure, when compared to the LAI-2200. Such advantages have led to the progressive replacement of LAI-2200 measurements with DHP within the VALERI project (Baret *et al*, 2005).

- **LI-COR LAI-2000 and LAI-2200**

The LAI-2200 Plant Canopy Analyser (and its predecessor LAI-2000) calculates the effective PAI from radiation measurements collected below 490 nm with a fisheye optical sensor (148° field-of-view) (LI-COR, 2009). Measurements collected above and below the canopy are used to determine the transmission of light, through the canopy, at five view angles simultaneously (LI-COR, 2009). PAI estimates derived via the LAI-2200 are based on four assumptions (a) the foliage is black, that is, no radiation is transmitted or reflected by the vegetation; (b) the foliage elements are small in comparison to the area of view of each sensor ring; (c) the foliage is randomly distributed; and (d) the foliage is azimuthally randomly orientated, that is, the leaves face in all compass directions (LI-COR, 2009). The LAI-2200 also computes an effective clumping factor (Ryu *et al*, 2010) of the

canopy, which is an upper limit to the 'true' clumping factor indicating how much the canopy appears to depart from random distribution. Recently, a methodology was presented by (Chianucci *et al*, 2014), which improves the LAI-2200's ability to estimate clumping based on restricting the field-of-view with azimuth view caps to measure multiple angular segments at each location. Increasingly large corrections for foliage clumping are made as more restrictive view caps are utilised, based on the logarithm averaging that occurs at the scale larger than the sensors field-of-view (Ryu *et al*, 2010; Chianucci *et al*, 2014). Although the authors believe DHP methods comparatively offer greater efficiency for this method, only requiring one measurement per location, with the added advantage of applying multiple clumping retrieval methods (Leblanc *et al*, 2014).

The LAI-2200 configuration enables measurements in a range of canopies with methodological approaches utilising one or two LAI-2200 sensors attached to a single data logger (LI-COR, 2009). Measurements can be collected under a variety of sky conditions. However, diffuse lighting conditions such as those present at dawn and dusk as well as when the sky is uniformly overcast, represent the optimal operational conditions (LI-COR, 2009). If measurements are taken under non-diffuse conditions then an underestimation of the measured effective LAI of up to 20% can result from multiple scatterings of light radiation as it passes through the plant canopy. Even though multiple scattering effects can be corrected (see Leblanc and Chen, 2001, who were able to reduce the error in LAI<sub>e</sub> measurements to within 2% and recommend the adoption of their methodology when collecting LAI measurements under non-diffuse conditions), it can be time consuming and require extensive calibration efforts therefore diffuse lighting conditions are recommended.

- **AccuPAR ceptometer**

The AccuPAR ceptometer measures the incident and transmitted photosynthetically active radiation (PAR). The device is optimal for low and regular canopies (Breda, 2003). The ceptometer integrates instantaneous fluxes of PAR radiation along a probe or wand which consists of a series of sensors sensitive to wavelengths in the region of 400-700 nm (White *et al*, 2000; Breda, 2003). Measurements are repeated both above and below the canopy in order to characterise incident and transmitted PAR. Ceptometer measurements should, ideally, be collected in bright sunny conditions within one hour of solar noon (White *et al*, 2000).

- **Tracing Radiation and Architecture of Canopies (TRAC)**

The TRAC instrument (3<sup>rd</sup> Wave Engineering, Ontario, Canada) differs from those instruments outlined above in that it measures both the canopy gap fraction and canopy gap size distribution. Gap fraction, as previously outlined, is the proportion of gaps within a canopy at a given solar angle. Conversely, gap size is the physical dimension of the gaps between individual elements (Gower *et al*, 1999; LeBlanc *et al*, 2002).

As stated previously, the spatial distribution of leaves within a canopy cannot be assumed to be random. This is a direct consequence of foliage clumping. As a result, measurements based on an assumption of a random spatial distribution can underestimate LAI (Chen *et al*, 1997). Chen *et al* (1997) demonstrate that gap size information can be related to the clumping index of a canopy hence the inclusion of this parameter within the TRAC device.

The TRAC device is based on the assumption that, as a consequence of non-random elements, the gap size distribution of a canopy contains multiple gaps. As the gap size distribution of a random canopy is known, gaps resulting from non-randomness can be identified and excluded from the total gap fraction accumulation; the gap fraction usually measured from radiation transmittance (LeBlanc *et al*, 2002). The difference between the measured gap fraction and gap fraction derived subsequent to non-random gap removal is subsequently utilised to quantify foliage clumping within the canopy (LeBlanc *et al*, 2002). This clumping index then enables conversion of the effective PAI to PAI (Chen *et al*, 1997).



- **Plant Canopy Imager CI-110**

The CI-110 (CID Bio-Science, Camas, WA USA) is a similar instrument to DHP, but with lower resolution and an interface that enables the user to simultaneously capture wide-angle (hemispherical) plant canopy images and estimate PAI and PAR levels from a single canopy scan (Figure 6.3).



**Figure 6.3** CI-110 canopy analyser. Photo on top shows measurements being acquired along a SLATS transect while photo below shows the graphical user interface of the instrument (note LAI measurement given on top left).

The CI-110 is a passive self-levelling imaging sensor. It has a 180° FOV (field of view) and a 24 sensor PAR wand used to measure the amount of incident solar radiation in the visible spectrum. The sensor is GPS enabled and can be used under any sky conditions (even varying lighting conditions) due to the integrated optical filter that ensures that scattered radiation does not affect the sensor by restricting radiation above 490 nm. This minimises the effect of light scattered by foliage and allows measurements to be conducted from below or within the canopy under varied light conditions (CID Bio-Science Inc., 2012).

PAI, canopy transmission coefficients and mean leaf angle are calculated by the external CI-110 computer software from the gap fraction inversion procedure (Norman and Campbell, 1989). Although, inversion

techniques where more than one variable is unknown should be treated with caution, such as in the previous example with both PAI and leaf inclination unknown. It is possible to calculate the PAI from a single image, however it has been found that a more accurate result is obtained for a field site when several readings and an average is taken. A recent comparison with high-resolution DHP methods was undertaken by Woodgate *et al.* (under review, AFM), which suggested that instruments unable to standardise exposure could cause issues for accurate  $P_{gap}$  from classified images in a range of forest environments and optimal lighting conditions. Advantages of high-resolution DHP cameras utilising RAW imagery have also been highlighted for more accurate classification of images (Jonkheere *et al.*, 2005; Macfarlane *et al.*, 2014).

- **Alternative approaches – Terrestrial Laser Scanning (TLS)**

In addition to the instruments outlined above, there is an increasing utilisation of active measurement techniques to estimate LAI. Such approaches are exemplified by the ground-based laser system, Echidna (Jupp *et al.*, 2008) and many other similar commercial terrestrial laser scanners (such as the FARO Focus 3D 120, the Leica C10, Leica HDS7000 and the Riegl VZ1000). An advantage of active sensors such as terrestrial laser scanners is their relative insensitivity to lighting conditions, and additional measurement of range (Newnham *et al.*, 2012). To compute the PAI from a ground-based laser scan, knowledge of the gap probability is required. The gap probability is defined as the probability of a gap appearing between the exit point of the sensor and the ‘target’ as a function of zenith angle ( $\theta$ ) and height above ground level ( $z$ ) (Jupp *et al.*, 2008). This can be computed from the laser scan itself. The gap probability is then expressed as:

$$P_{gap}(z, \theta) = e^{-G(\theta)PAI(z)/\cos(\theta)} \quad P_{gap}(z, \theta) = e^{-G(\theta)LAI(z)/\cos(\theta)} \quad (\text{equation 6.9})$$

equation 5 is similar to equation 1, however in this case,  $LAI(z)$  is the best estimate based on measurements of  $P_{gap}(z, \theta)$  from multiple zenith rings, where  $G(\theta)$  is the fraction of the leaf area projected on a plane normal to the zenith angle  $\theta$  (Ross  $G$  function; Ross, 1981). This allows no separation of foliage and woody vegetation, so it is assumed that plant area index (PAI) is equal to the LAI. Although a correction for the proportion of woody material can be conducted post-hoc. To calculate the PAI from equation 5, the equation is simply inverted (Strahler *et al.*, 2008):

$$PAI(z) = -\frac{\ln P_{gap}(z, \theta) \cos(\theta)}{G(\theta)} \quad LAI(z) = -\frac{\ln P_{gap}(z, \theta) \cos(\theta)}{G(\theta)} \quad (\text{equation 6.10})$$

A number of alternative methods to derive PAI have been suggested. These are primarily based on gap probability theory (e.g. Hosoi *et al.*, 2007; Béland *et al.*, 2014; Moorthy *et al.*, 2008; Huang & Pretzsch 2010). However, TLS remains challenging for large-area PAI characterisation due to (i) the high cost of commercial instruments, (ii) the limited scanning efficiency (caused by environmental factors combined with size and weight of instruments, and limited instrument capabilities of data processing, storage and battery life), and (iii) the ill-posed nature of the lidar beam interaction with canopy elements (Béland *et al.*, 2014; Hancock *et al.*, 2014).

TLS limitations are progressively being overcome with the development of new scanners and collaboration between researchers, both in the research and commercial domains. For example, the latest ECHIDNA design (Dual-Wavelength ECHIDNA Lidar – DWEL) incorporates two lasers of different wavelength that produce a vegetation index from the intensity of the reflected laser energies. This allows the vegetation to be both structurally and functionally assessed. This design also enables the separation of woody and non-woody vegetation material thus allowing the true LAI value to be calculated.



Furthermore, collaborative research groups such as the Terrestrial Laser Scanner International Interest Group (TLSIIG) are undertaking activities to further the understanding and application of TLS for assessment and monitoring of vegetation dynamics and parameters (TLSIIG, 2014 or WWW2).

### ***Canopy-analysers comparison: LAI Estimation***

The footprint of each of the outlined canopy analysers varies as a function of (a) the device utilised; and (b) the canopy sampled. For example, when utilising the LAI-2200 and DHP, with observations between 60 and 70 degrees from the zenith, the footprint of the instruments will correspond to a 150 metre diameter disk in forests (up to 40 metres in height). Conversely, in very short canopies the footprint is reduced to less than 2 metres (Morisette *et al*, 2006). For the AccuPAR and TRAC devices, the footprint is dependent upon the sun zenith angle and tree height (Morisette *et al*, 2006). Equally, in comparison to other instruments, the TRAC device is based on a measurement transect and will therefore result in a rectangular footprint. The length of this footprint is determined by the transect length, the width by the solar angle and canopy height (Morisette *et al*, 2006).

Several authors report the underestimation of PAI via indirect measurement techniques, a consequence of the non-random distribution of foliar elements within the canopy and therefore violation of the assumptions supporting PAI estimation (Chen *et al*, 1997; Breda, 2003). As stated previously estimates of spatial clumping, inferred from the gap size distribution, can be utilised in the conversion of effective PAI to PAI as demonstrated by the TRAC instrument (Chen *et al*, 1997). However, given the complexity of measuring canopy gap size distribution (and its reliance on a TRAC instrument) simplified measures of clumping index have been derived based on (a) the ratio of the crown depth to crown diameter (Gower *et al*, 1999); and (b) an estimate of gap size distribution as derived from DHP (cf. Leblanc *et al.*, 2014).

A further discrepancy between direct and indirect LAI estimates, specific to woody vegetation types, is the result of indirect methods calculating PAI as opposed to LAI. This is a direct consequence of optical techniques including non-green elements, that is, woody branches and stems in LAI measurements. The accurate measurement of LAI therefore requires the calculation of contributions from woody vegetation elements (Chen *et al*, 1997; Breda, 2003). Multiple methodologies for the derivation of LAI from PAI are proposed in the research literature (see **section 6.2.2 Correction for the proportion of woody material ‘ $\alpha$ ’** and Breda (2003) for a comprehensive review).

The spatial and temporal relevance of ground-based LAI measurements is an important consideration (Breda, 2003). For example, the timing of sampling should consider seasonal (natural and incident) variation in LAI (Breda, 2003). Equally, the spatial variability of the canopy will influence the required number and spatial arrangement of LAI measurements. When LAI is estimated indirectly from gap fraction or radiation attenuation measurements, the number of measurements required to estimate LAI with a given accuracy is a function of canopy heterogeneity (Gower *et al*, 1999). Another key consideration is which zenith angles are to be used for analysis from indirect instruments. As previously discussed, PAI can be inverted over a range of zenith angles, or a single zenith angle, which in turn affects the sampled canopy proportion, with higher zenith angles (60 degrees) sampling a larger area than near zenith.

Multiple studies compare LAI as derived from direct and indirect measurement techniques (Whitford *et al*, 1995; Gower *et al*, 1999; White *et al*, 2000; Breda, 2003; Coops *et al*, 2004). Gower *et al* (1999) concluded that overall, direct and indirect estimates of LAI were within 25 to 30% for most canopies. Although, it should be noted that improvements to indirect LAI retrieval techniques and methodologies have been made since. However, the authors note that indirect estimates of LAI reach asymptote at approximately five or six. This is in comparison to direct measurements which reached a LAI of nine in the study area. The authors conclude that the saturation of gap fraction techniques at LAI values approaching five or six necessitates the direct measurement of LAI for

canopies expected to have LAI values greater than this threshold (Gower *et al*, 1999). This finding warrants further research utilising the latest independent structural parameters retrieval methods.

### **6.2.3 Recommendations and areas for improvement**

A comparison of current LAI validation programs as shown in Table 6.3 suggests that indirect techniques are primarily used for the ground-based estimation of LAI. This is because indirect techniques can measure large areas of land more efficiently than direct techniques. LAI is typically estimated via four optical instruments (a) the LAI-2200 plant canopy analyser; (b) the AccuPAR ceptometer; (c) digital hemispherical photography (DHP) and (d) the Tracing Radiation and Architecture of Canopies (TRAC) instrument (Table 6.3).

Although utilised, the inclusion of destructive (direct) LAI measurements is limited. Equally, it should be noted that multiple validation programs include more than one LAI estimation technique (Table 6.3). Such a trend was reflected in the BigFoot project which utilised (a) direct measurements including periodic harvest for non-forest sites and the application of allometric relationships at forested sites and (b) indirect LAI estimation techniques, LI-COR LAI-2000 as a function of vegetation type and date (Morissette *et al*, 2006). In an Australian context, Hill *et al* (2006) estimated LAI, via ground-based measurements, using (a) hemispherical photography at a tropical rainforest site in North Queensland; (b) LI-COR measurements in remnant forests within New South Wales; and (c) tree and understory hemispherical photography in both central Queensland and North East Victoria.

Given the variety of techniques and instruments available for measuring LAI, the most appropriate instrument is likely to be a function of the canopy structure and study area characteristics (White *et al*, 2000). Jonckheere *et al* (2004) conclude that an ideal device for measuring LAI should (a) be a hemispherical sensor that simultaneously measures the canopy gap fraction at a range of zenith angles, thus ensuring a more efficient sample than can be achieved with linear sensors; (b) permit the derivation of gap size distribution in order to provide information on leaf clumping; (c) enable the identification of green and non-green canopy elements; and (d) permit a characterisation of LAI over low vegetation canopies by looking downwards. The authors conclude that such characteristics can be achieved using a hemispherical camera based approach.

Areas for continued research are the standardisation of (a) field approaches for DHP data collection; (b) segmentation/classification into green and non-green elements; (c) the computation of the woody projection function (Woodgate *et al*, in review RSE), and (d) the definition of appropriate exposure, spectral, radiometric and spatial resolution settings required to ensure rigorous data collection (Jonckheere *et al*, 2004; Macfarlane *et al.*, 2014).

### **6.2.4 Australian canopies and LAI**

Hill *et al* (2006) state that in Australia all satellite, airborne, or ground-based measurements of LAI are influenced by the leaf inclination of the *Eucalyptus* species which tend to range between 60 and 80 degrees. As a result, ground-based measurements of LAI derived from gap fraction, plant canopy analysers, camera-based point quadrats and hemispherical photographic techniques all produce biased estimates (Coops *et al*, 2004). Research has demonstrated that such biases are potentially larger in sparse canopies (Whitford *et al*, 1995). This is an important consideration given 78% of native forests in Australia (which represent an estimated 147.4 million hectares) are Eucalypt species (ABARES, 2012). Consequently, the authors suggest that indirect (optical) methods of LAI estimation require calibration, via direct LAI measurement, to produce accurate estimates of canopy LAI within Australian ecosystems (Coops *et al*, 2004).

Equally, as a consequence of this vertical leaf inclination and a higher proportion of radiation transmittance to the forest floor, Hill *et al* (2006) conclude that projected foliage cover, when adjusted for woody canopy elements, may provide a better correlation with satellite based LAI products.

## 6.3 $F_{APAR}$ Validation

---

A review of LAI validation programs demonstrates that  $f_{apar}$  and LAI are associated metrics which are frequently validated coincidentally. This is exemplified by the VALERI and BigFoot projects which both estimate  $f_{apar}$  in and LAI in conjunction.

### 6.3.1 *In situ fapar Measurements*

Weiss and Baret (2011) suggest that there are four *in situ* methods of quantifying the  $f_{apar}$  at the local scale: the use of quantum sensors that measure all the terms of the radiation balance; instantaneous PAR transmittance measurements; directional measurements using LAI-2200, DHP or LiDAR; and finally describing the 3D optical elements of the canopy as realistically as possible and then simulating the  $f_{apar}$ . However, the most common *in situ*  $f_{apar}$  measurements that are used are calculated from the difference in photosynthetically active radiation (PAR) entering and leaving the canopy, that is, PAR absorption, divided by the incoming PAR ( $f_{IPAR}$ ).

Many *in situ* sensors such as the LAI-2200, lidar, DHP, AccuPAR ceptometer and other ceptometers can be used to calculate the  $f_{IPAR}$ . However, care must be taken when using such measurement devices. Asner *et al* (1998) mentioned that  $f_{IPAR}$  underestimates  $f_{apar}$  by about 3-10 % for canopies containing dense green materials while these underestimations rise to levels of around 10-40% when considering shrublands and woodlands with LAI < 3.0.

The BigFoot project estimates  $f_{apar}$  via two techniques, firstly, from the DIFFN variable provided by the LI-COR LAI-2200 and, secondly, from a continuous PAR tram system (WWW3). The PAR tram system measures incident and transmitted PAR both above and below the canopy at increments along a 30 metres track (BigFoot Website).

Fensholt *et al* (2004) collected ground-based measurements of  $f_{apar}$  (and LAI) at a series of grassland savannah sites in order to validate MODIS derived  $f_{apar}$  data products.  $f_{apar}$  is measured with a SKYE PAR Quantum sensor (Fensholt *et al*, 2004). Fensholt *et al* (2004) derived daily averages of  $f_{apar}$  by repeating measurements at 10 minute intervals between 9am and 3pm. The authors utilised repeated measurements over a large range of solar zenith angles, so to minimise errors introduced by the correction factor  $G$ , a function introduced into  $f_{apar}$  derivation to account for non-random leaf angle distributions (Fensholt *et al*, 2004). Sensitivity analysis demonstrated that measurements averaged over this time period were representative of 10.30am and 10.30pm values and therefore compatible with MODIS derived  $f_{apar}$  measurements (Fensholt *et al*, 2004).

The ratio of the incident PAR recorded above and below the canopy is closely related to canopy gap fraction. This measure is therefore influenced by sun zenith angle, the amount of diffuse radiation and canopy clumping (Gower *et al*, 1999). Other error sources in the ground-based estimation of PAR include: (a) variation in the soil albedo; (b) the  $f_{apar}$  model assumptions; and (c) uncertainty in LAI measurements. The last is relevant only if PAR is being derived from LAI as opposed to being directly measured (Fensholt *et al*, 2004).

## 6.4 Exemplar methodology for the validation of satellite LAI products in Australia using an up-scaling approach

The validation of specific satellite remote sensing products has been the focus of many research groups and programs in the past (Table 6.3). The AusCover facility within TERN is currently validating the MODIS Collection 5 LAI product for the Australian continent. The validation of this product is a multi-step process involving current *in situ* field measurements, historical LAI data, intermediate resolution measurements (such as airborne laser scanning or ALS). This is followed by the up-scaling of *in situ* measurements to moderate resolution (on the order of 1km<sup>2</sup>) using intermediate measurements (e.g., Landsat imagery).

Due to the enormity of Australia, it is imperative that reference data used to validate the MODIS LAI product is collected from multiple locations and ecosystems across the continent. Accordingly, AusCover utilises data collected from eight TERN calibration/validation supersites around Australia in conjunction with data collected by other TERN nodes such as AusPlots Rangelands (WWW4), and historical LAI records, such as those contained in Hill *et al.*, 2006.

*In situ* LAI measurement techniques that are most commonly used by AusCover field teams at the calibration/validation sites include digital hemispherical photography and plant canopy analysers (such as LAI-2200 and CI-110). At each of these calibration/validation supersites, ALS has been flown, from which the effective LAI can be derived using a Beers Law inversion of the gap fraction. This provides a means of up-scaling the *in situ* measurements (via a transfer function) to a moderate resolution, similar to that achieved using MODIS.

At the AusCover calibration/validation supersites, ground-based LAI measurements are typically collected along the SLATS Star transect at 25 m intervals (WWW5) (Figure 6.4). Typically there are about five to seven SLATS transects per 5km by 5km supersite.

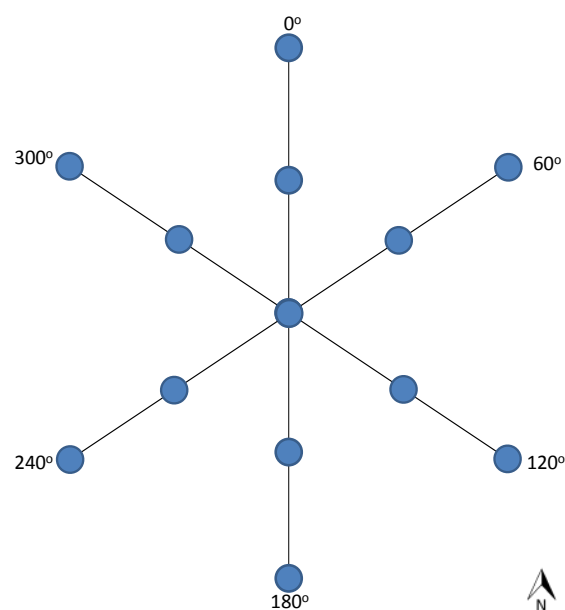


**Figure 6.4** SLATS Star Transect representing a single validation field site or plot. Each transect segment is 100 m in length with the blue representing locations where hemispherical photos were taken.

LAI measurements using hemispherical photography and plant canopy analysers are best captured under completely diffuse lighting conditions such as uniform overcast skies or at dawn/dusk. Steps followed by AusCover field teams to measure and validate LAI are described below. These are recommended to be taken under diffuse lighting conditions.

### **6.4.1 Digital Hemispherical Photography (DHP)**

1. **Sampling Design:** At each SLATS site or plot, DHP are taken at 13 locations: 1 in the centre of the star transect, 6 half way along each arm (at 25 m from centre), and 6 at the ends of each transect (indicated by the blue dots in Figure 6.4).
2. **Image Capture:** Ensure that the camera is near level for each of the photographs and that the top of the photograph (top of the camera) faces magnetic north to simplify post processing of the images.
3. Typically images are taken at breast height (1.30 m above the ground surface). However, if understory is present, it is good practise to take photographs from above and below the understory. For grassy ecosystems, if possible it is encouraged to take photographs from ground level as well as above the ground looking down. Note: images are recommended to be taken at least  $\pm 1$  m away from large tree stems, as a distance less than this threshold may bias the gap fraction, clumping, and PAI from unrepresentative images. If the measurement locations will be used for monitoring purposes, then permanent markers are recommended to be placed at each of the measurement locations. For the full AusCover digital hemispherical photography protocol, refer to the AusCover wiki (WWW6).
4. Ensure the camera is taking high quality format jpeg images in addition to storing RAW format. The choice of RAW or in-camera jpeg image format is important for the post-processing stage of image classification. Enable the camera bracketing function and set to  $\pm 1$  f-stop. This ensures that three differently exposed images can be captured efficiently. Set the exposure metering to matrix metering, which utilises the entire camera scene within the viewfinder to assess the appropriate metering. Set the exposure program of the camera to Aperture Priority. The choice of exposure level is a manual and iterative approach, following the guidelines of Beckschäfer *et al*, (2013). At each location, take a photo (automatic exposure is good starting point) and (i) in preview mode look at the image for overexposure (most likely at zenith if diffuse lighting) and for clear separation of foliage and sky in the bright parts of the image, and (ii) check the histogram of the image to ensure there are few pixels with maximum digital number value (indicating overexposure). Ideally, the sky pixels peak is located just below the maximum histogram value. If the image is overexposed, reduce the shutter speed and vice versa. Repeat the process until this criteria has been satisfied. This will create measurement redundancy in the image capture process. If the RAW format is used for post-processing, then additional firmware can be installed on some cameras that enable the preview of the RAW histogram, such as Magic Lantern (ref <http://www.magiclantern.fm/>) or the Canon Hack Development Kit (WWW ref -<http://chdk.wikia.com/wiki/CHDK>). Although the RAW image format is less sensitive to camera exposure level due to greater dynamic range (or bit-depth), it is still important to ensure the images are not over- or under-exposed as the lost detail cannot be recovered in post-processing stages. Otherwise shooting the camera 1 stop under automatic exposure is recommended (Macfarlane *et al*, 2014).
5. ISO is essentially the camera's sensitivity to light. Low ISO values tend to be preferred given they increase the signal to noise ratio. For camera stability, it is highly recommended to use low ISO values (100-400) in conjunction with a tripod (and remote trigger). This will lead to a reduction in mixed pixels and a more

accurate image classification. The ISO value should only be increased if the shutter speed is very long (e.g. > 0.5 seconds) – as wind and camera movement can cause blurring in the image.

6. **Post Processing:** There are a number of post-processing methods to classify the images and subsequently derive canopy structural metrics. Two exemplar processes are outlined below; one for the RAW image format, and one for the in-camera jpeg format. The advantage of the RAW image processing method is that it was shown to be almost insensitive to camera exposure (Macfarlane *et al*, 2014). Whereas in-camera jpeg format image classification is very sensitive to camera exposure, thus leading to significantly different structural metric estimations. It is important to note that camera and lens calibration parameters (i.e. the lens projection centre or 'offset' and lens projection function or 'radial distortion') need to be known to for the post-processing stages.

**Method 1 (RAW):** The RAW imagery can be processed in a number of stages, combining three software packages to produce canopy openness, gap fraction, PAI and canopy element clumping metrics. The stages are as follows:

- A. **Image format conversion:** Convert the RAW imagery into 8 bit jpeg format for further analysis, using an updated method outlined in Macfarlane *et al*, (2014). This stage involves an automated process utilising the open source software functionality of dcrw (WWW ref: <https://www.cybercom.net/~dcoffin/dcrw/>); please contact Craig Macfarlane ([craig.macfarlane@csiro.au](mailto:craig.macfarlane@csiro.au)) for a compilation.
- B. **Image classification:** The subsequent steps are applicable to both in-camera jpegs and the converted RAW to jpeg formats. The DCP toolbox v3.14 (Macfarlane 2011; Macfarlane *et al*, 2014, [craig.macfarlane@csiro.au](mailto:craig.macfarlane@csiro.au)), has in-built functionality to automate the image classification process. Key outputs of this step include a binary classified image, and a report of canopy openness and proportions of mixed pixels. The lens projection centre (coordinates) and image diameter are required input settings.
- C. **Intermediate step to compute canopy element clumping:** Utilising the classified images from Step 2, input them into DHP.exe to compute TRAC instrument-like profiles for input into the TRACWin.exe software (contact Sylvain Leblanc for a copy of both DHP.exe and TRACWin.exe, ([Sylvain.LebLANC@nrcan-rncan.gc.ca](mailto:Sylvain.LebLANC@nrcan-rncan.gc.ca))). It is recommended to compute a single TRAC-like profile per plot of images.
- D. **Canopy element clumping,  $PAI_e$ , PAI, and LAI:** Use the TRAC-like profiles created in DHP.exe as input into TRACWin.exe to compute canopy element clumping and PAI. Batch mode can be utilised for efficient processing of plots. The in-built CLX clumping method with a segment size of 15 degrees is recommended, please refer to Leblanc et al. (2014) for further information. Note: a post-hoc correction for the lens projection function may be required, due to the default linear projection function assumed in DHP.exe and TRACWin.exe. If the scene G function is unknown, i.e. the angular distribution of wood or leaf elements have not been quantified, then the 55-60 degree zenith angle range is recommended to use for the clumping metric due to the G projection function of leaf and wood converging to be equal 0.5 at that angle. Clumping at  $\theta \approx 57.3$  degrees can combined with the known G ( $\approx 0.5$ ), and  $PAI_e$  estimated from the average  $P_{gap}$  at the same zenith angle range using Eqn. 6.4 to compute PAI. A correction for the proportion of woody material to plant material ' $\alpha$ ' can also be made if available to convert PAI into LAI (Eqn. 6.3).

**Method 2 (in-camera jpeg):** Photographs from each site are post processed using CAN-EYE imaging software (Weiss and Baret, 2010). CAN-EYE is used to extract LAI, average leaf inclination angle (ALA), fraction of absorbed photosynthetically active radiation (FAPAR), vegetation cover fraction (FCOVER) and bidirectional gap fraction. It is also possible to use CAN-EYE with pre-classified images from the RAW format, which have been re-formatted to jpeg.

The exact process used to calculate the effective LAI and true LAI from the DHP images using the CAN-EYE software is set out step-by-step in the CAN-EYE user manual (Weiss and Baret, 2010). However, a schematic diagram of the general classification process is provided in Figure 6.5.

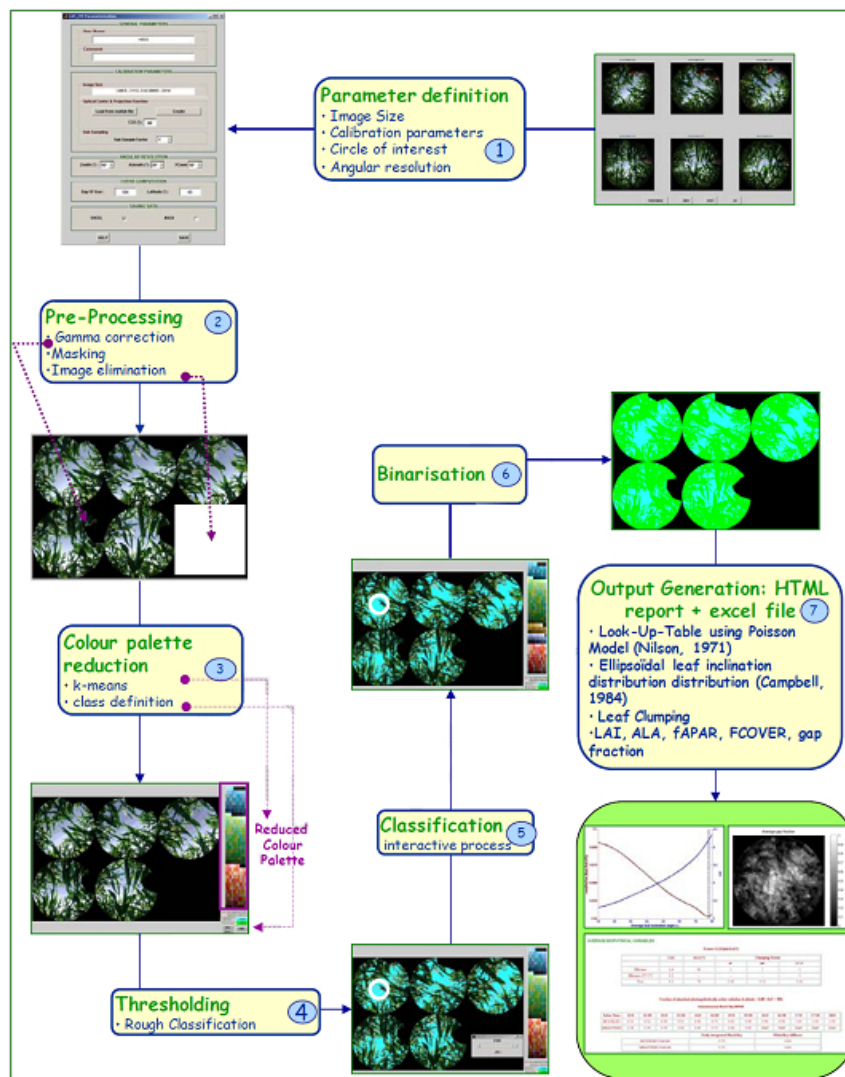


**Figure 6.5** Schematic diagram representing the general process where-by images are processed and LAI is calculated using the CAN-EYE imaging software (image extracted from Weiss and Baret, 2010).

### 6.4.2 Plant Canopy Analyser – LAI-2200

1. Upon commencing measurements, be sure to record an 'above canopy' reference measurement in a clearing. The sensor wand is then switched into 'below canopy' mode so that the LAI measurements can be made. LAI-2200 measurements are to be taken at the same positions as the DHP measurements at regular intervals along each of the 100 m transects, ideally with a GPS logger attached to the LAI-2200 console to record the position. If a GPS logger is not available then the correct procedure is as follows.
2. Measurements are to be taken along each transect arm in the same order and direction as the star transect point intercept measurements were taken.
3. Take measurements at regular specified intervals.
4. Record each transect as a separate file with the transect name and measurement interval (e.g. chow01\_transect1\_5m). For the full AusCover LAI-2200 protocol, refer to the AusCover wiki and the LAI-2200 user manual which outlines the full methods to be used in different vegetation types (WWW7, and Licor, 2009).

### 6.4.3 Terrestrial Laser Scanning (TLS)

5. At each of the calibration/validation field sites, TLS measurements are also recorded (Figure 6.6) along each SLATS plot. As each TLS produces a 360° FOV point cloud of the immediate area of ground and canopy, a modified SLATS star transect is used.



**Figure 6.6** Recording TLS measurements and metadata in the field using a Riegl Laser Scanner.

6. A total of five TLS scans are taken per SLATS plot (Figure 6.7): 1 scan taken at the centre followed by 4 scans taken approximately 35 m from the centre along each of the NE, SE, SW and NW transect arms. By using this spatial configuration of scans, a complete characterisation of the structural properties of the vegetation can be made.

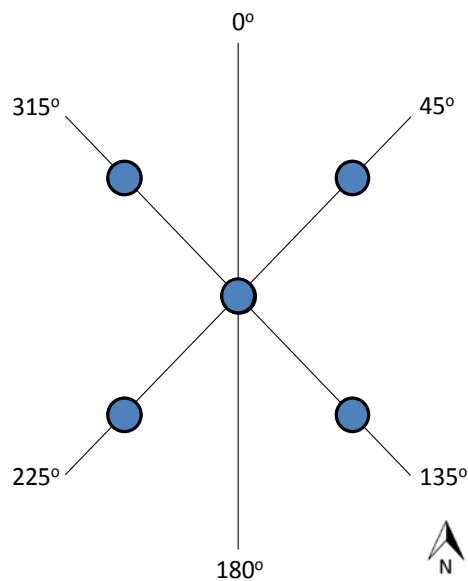


**Figure 6.7** Modified SLATS Star Transect representing a single validation field plot. Each of the blue dots indicates a TLS measurement position, allowing for a complete site characterisation of the vegetation structure to be made using this spatial configuration.



7. Once all the in situ vegetation measurements (DHP, TLS and plant canopy analyser) at each plot site have been recorded, post processing and collation of the data is carried out.

#### 6.4.4 Up-scaling of the in situ LAI measurements

To compare with or validate a moderate resolution satellite product (such as the MODIS Collection 5 LAI product), *in situ* measurements must be up-scaled via the use of high resolution satellite imagery or airborne Lidar data (Morisette *et al.*, 2006). AusCover will primarily use Landsat imagery to up-scale the *in situ* measurements, however both up-scaling methods will be assessed where airborne lidar (ALS) is available. The process implemented to up-scale *in situ* measurements is set out below:

##### **When Using Satellite Imagery**

8. The direct validation approach (Morisette *et al.*, 2006) consists in using high spatial resolution imagery (on the order of 20 - 30 m) to scale the ground LAI measurements up to a moderate resolution pixel size (approximately 1km x 1 km). For this, a “transfer function” between high spatial resolution surface reflectance and LAI measurements is established.
9. The transfer function is applied to an appropriate extent of the high spatial resolution image (for the AusCover/TERN supersites, a 100 m x 100 m tile size is used).
10. The resulting high spatial resolution LAI map is aggregated up to a coarser pixel size for comparison with moderate resolution products such as MODIS.

##### **Using Airborne Laser Scanning (ALS)**

11. The ALS LAI is calculated using the intensity model described by Hopkinson and Chasmer (2007). This involves calculating gap fraction grids for the field site area with the same resolution as the satellite imagery that is used (namely Landsat imagery with 30 m pixel size).
12. Gap fraction grids are calculated in their simplest form by taking a ratio of the below canopy returns to the total number of ALS returns for a given grid cell size. This results in an index of canopy gaps (P).
13. A simple Beers Law inversion is then applied to obtain the effective LAI;

$$LAI_e = -\frac{\ln(Pgap)LAI_s}{k} = -\frac{\ln(P)}{k} \quad (\text{equation 6.11})$$

Where *Pgap* is the gap fraction and *k* is the site dependent extinction coefficient.

14. The resulting  $LAI_e$  grid can then be used in the same manner as the satellite imagery to up-scale the *in situ* LAI measurements. A transfer function between the *in situ* and ALS measurements is applied, and the resulting high resolution LAI map is aggregated up to a coarser pixel size to be compared directly with moderate resolution products (e.g. Figure 6.8).

MOD15A2 MODIS/Terra Gridded 1KM Leaf Area Index LAI (8-day composite) (m<sup>2</sup> plant / m<sup>2</sup> ground)  
 MOD15A2.2012.105.aust.005.b02.1000m\_lai.hdf

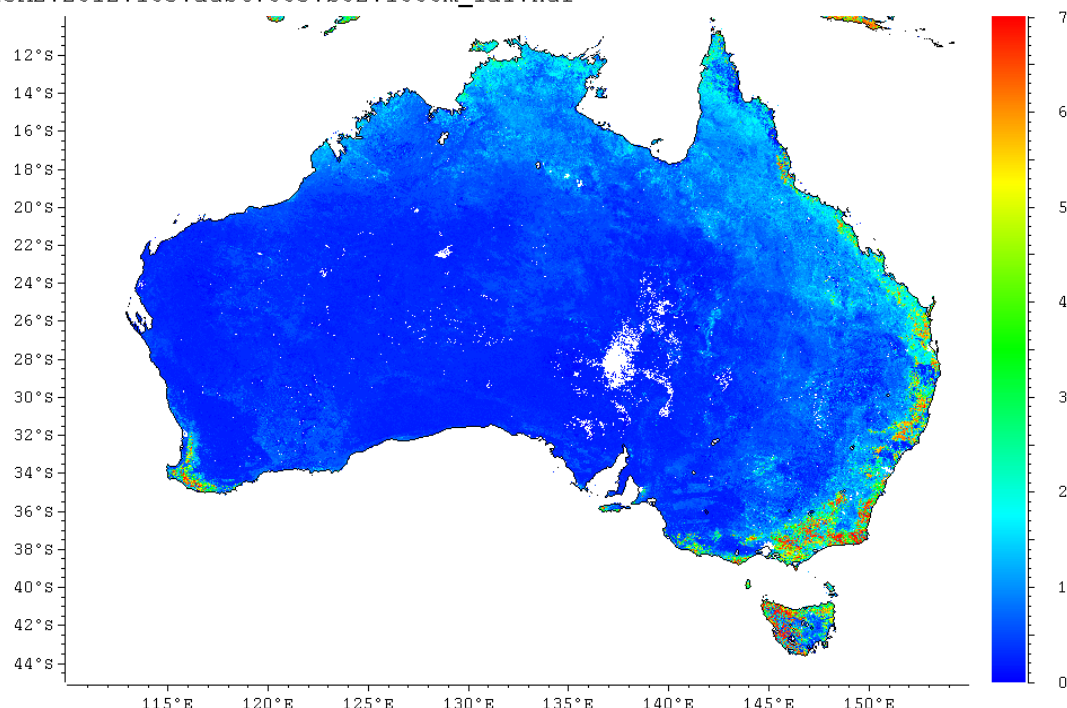


**Figure 6.8** MODIS Collection 5 LAI product. Gridded 1 km x 1 km, 8-day composite product for Australia, acquired using the MODIS Terra sensor (image source WWW8).

The use of these two up-scaling methods (satellite imagery and ALS) in conjunction with a suite of *in situ* measurements and historical data will allow TERN AusCover to successfully validate the MODIS Collection 5 LAI product on a continental scale.

## References

- ABARES, 2012. Australia's forests at a glance 2012, ABARES, Canberra, August. Available at [http://adl.brs.gov.au/data/warehouse/9aaf/9aafe003/fag12d9aafe003201208/ForestsAtGlance\\_2012\\_v1.0.0.pdf](http://adl.brs.gov.au/data/warehouse/9aaf/9aafe003/fag12d9aafe003201208/ForestsAtGlance_2012_v1.0.0.pdf).
- Asner, G. P., Wessman, C. A. and Archer, S. (1998) Scale dependence of absorption of photosynthetically active radiation in terrestrial ecosystems. *Ecological Applications* **8** 1003-1021.
- AusCover Wiki (2013). <http://data.auscover.org.au/xwiki/bin/view/Main/>
- Baret, F., Weiss, M., Allard, D., Garrigues, S., Leroy, M., JeanJean, H., et al. (2005) VALERI: a network of sites and a methodology for the validation of medium spatial resolution land satellite products, *Remote Sensing Environment* (Accessed at <http://w3.avignon.inra.fr/valeri/documents/VALERI-RSESubmitted.pdf> - August 2010).
- Beckschäfer, P, Seidel, D, Kleinn, C, & Xu, J. (2013). On the exposure of hemispherical photographs in forests. [On the exposure of hemispherical photographs in forests]. *iForest - Biogeosciences and Forestry*, 6(4), p. 228-237. doi: 10.3832/for0957-006
- Béland, M., Baldocchi, D. D., Widlowski, J-L., Fournier, R A., & Verstraete, M. M. (2014). On seeing the wood from the leaves and the role of voxel size in determining leaf area distribution of forests with terrestrial LiDAR. *Agricultural and Forest Meteorology*, 184(0), p. 82-97. doi: <http://dx.doi.org/10.1016/j.agrformet.2013.09.005>
- BigFoot Website: <http://www.fsl.orst.edu/larse/bigfoot/overview.html> (Accessed August 2010)

- Bréda, N.J.J. (2003). Ground-based measurements of leaf area index: a review of methods, instruments and current controversies, *Journal of Experimental Botany*, 54(392) p.2403 - 2417.
- CEOS. (2014). Global LAI Product Validation Good Practices v2.0. In R. Fernandes, S. Plummer & J. Nightingale (Eds.).
- Chen, J.M., & Cihlar, J. (1995). Quantifying the effect of canopy architecture on optical measurements of leaf area index using two gap size analysis methods. *Geoscience and Remote Sensing, IEEE Transactions on*, 33(3), 777-787. doi: 10.1109/36.387593
- Chen, J.M., Rich, P.M., Gower, S.T., Norman, J.M. & Plummer S. (1997). Leaf area index of boreal forests: theory, techniques and measurements, *Journal of Geophysical Research*, 142 (D24), p. 29,429-29,443.
- Chianucci, F., Macfarlane, C., Pisek, J., Cutini, A., & Casa, R. (2014). Estimation of foliage clumping from the LAI-2000 Plant Canopy Analyzer: effect of view caps. *Trees*, 1-12.
- CID Bio-Science Inc. (2012). *Plant Canopy Imager CI-110 Instruction Manual, Version 5.0.3*, CID Bio-Science Inc., Camas, WA USA.
- Coops, N.C., Smith, M.L., Jacobsen, K.L., Martin M. & Ollinger, S. (2004). Estimation of plant and leaf area index using three techniques in a mature eucalypt canopy, *Austral Ecology*, 29 p. 332 - 341.
- Cohen, W.B., Maersperger T.K., Turner, D.P., Ritts, W.D., Pflugmacher, D., Kenned, R.E., Kirschbaum, A., Running, S.W., Costa, M. & Gower, S.T. (2006). MODIS Land Cover and LAI Collection 4 Product Quality Across Nine Sites in the Western Hemisphere, *IEEE Transactions on Geoscience and Remote Sensing*, 44 (7) p.1843 - 1857.
- Côté, J.-F., Widłowski, J.-L., Fournier, R.A., & Verstraete, M.M. (2009). The structural and radiative consistency of three-dimensional tree reconstructions from terrestrial lidar. *Remote Sensing of Environment*, 113(5), 1067-1081. doi: <http://dx.doi.org/10.1016/j.rse.2009.01.017>
- Danson, F.M., Gaulton, R., Armitage, R.P., Disney, M., Gunawan, O., Lewis, P., Pearson, G., & Ramirez, A.F. (2014). Developing a dual-wavelength full-waveform terrestrial laser scanner to characterize forest canopy structure. *Agricultural and Forest Meteorology*, 198–199(0), 7-14. doi: <http://dx.doi.org/10.1016/j.agrformet.2014.07.007>
- de Wit, C.T. (1965). *Photosynthesis of leaf canopies*: Centre for Agricultural Publications and Documentation.
- Fensholt, R., Sandholt, I & Rasmussen, M.S. (2004). Evaluation of LAI, fAPAR and the relation between fAPAR and NDVI in semi-arid environments using in-situ measurements, *Remote Sensing of Environment*, 91 p. 490 - 507.
- Gower, S.T., Kucharik, C.J. & Norman, J.M. (1999). Direct and Indirect Estimation of Leaf Area Index,  $f_{\text{apar}}$  and Net Primary Production of Terrestrial Ecosystems, *Remote Sensing of Environment*, 70 p. 29 - 51.
- Hancock, S., Essery, R., Reid, T., Carle, J., Baxter, R., Rutter, R., & Huntley, B. (2014). Characterising forest gap fraction with terrestrial lidar and photography: An examination of relative limitations. *Agricultural and Forest Meteorology*, 189–190(0), p. 105-114. doi: <http://dx.doi.org/10.1016/j.agrformet.2014.01.012>
- Hill, M.J., Senarath, U., Lee, A., Zeppel, M., Nightingale, J.M., Williams, R. & McVicar, T.R. (2006). Assessment of the MODIS LAI product for Australian ecosystems, *Remote Sensing of Environment*, 101 p. 495 - 518.
- Hopkinson, C. and Chasmer, L. (2007). Using discrete laser pulse return intensity to model canopy transmittance. *Photogrammetric Journal of Finland*, 20 (2) p. 16 – 26.
- Hosoi, Fumiki, & Omasa, Kenji. (2007). Factors contributing to accuracy in the estimation of the woody canopy leaf area density profile using 3D portable lidar imaging. *Journal of Experimental Botany*, 58(12), p. 3463-3473. doi: 10.1093/jxb/erm203
- Huang, P., & Pretzsch, H. (2010). Using terrestrial laser scanner for estimating leaf areas of individual trees in a conifer forest. *Trees - Structure and Function*, 24(4), p. 609-619.
- Jonckheere, I., Fleck, S., Nackaerts, K., Muys, B., Coppin, P., Weiss, M. & Baret, F. (2004). Review of methods for in situ leaf area index determination Part I. Theories, sensors and hemispherical photography, *Agricultural and Forest Meteorology*, 121 p. 19 - 35.
- Jupp, D.L.B., Culvenor, D.S., Lovell, J.L., Newsham, G.L., Strahler, A.H. & Woodcock, C.E. (2008). Estimating forest LAI profiles and structural parameters using a ground-based laser called Echidna, *Tree Physiology* 29 p. 171 - 181.

- Kucharik, C.J., Norman, J.M., Murdock, L.M., & Gower, S.T. (1997). Characterizing canopy nonrandomness with a multiband vegetation imager (MVI). *Journal of Geophysical Research: Atmospheres*, 102(D24), 29455-29473. doi: 10.1029/97JD01175
- Lambert, J. (1760). *Photometria, sive de Mensura et gradibus luminis, colorum et umbrae* (Augsberg: Eberhard Klett).
- Lang, A.R.G., & Xiang, Y. (1986). Estimation of leaf area index from transmission of direct sunlight in discontinuous canopies. *Agricultural and Forest Meteorology*, 37(3), 229-243. doi: 10.1016/0168-1923(86)90033-x
- Leblanc, S.G. & Chen, J.M. (2001). A practical scheme for correcting multiple scattering effects on optical LAI measurements, *Agricultural and Forest Meteorology*, 110 p. 125 - 139.
- Leblanc, S.G. (2002). Correction to the plant canopy gap-size analysis theory used by the Tracing Radiation and Architecture of Canopies instrument. *Applied Optics*, 41(36), 7667-7670.
- Leblanc, S.G., Chen, J.M., Fernandes, R., Deering, D.W., & Conley, A. (2005). Methodology comparison for canopy structure parameters extraction from digital hemispherical photography in boreal forests. *Agricultural and Forest Meteorology*, 129(3-4), 187-207. doi: 10.1016/j.agrformet.2004.09.006
- Leblanc, S.G., Chen, J.M. & Kwong, K. (2002). *Tracing Radiation and Architecture of Canopies: TRAC manual (Version 2.1.3)*, Natural Resources Canada.
- Leblanc, S.G., & Fournier, R.A. (2014). Hemispherical photography simulations with an architectural model to assess retrieval of leaf area index. *Agricultural and Forest Meteorology*, 194(0), 64-76. doi: <http://dx.doi.org/10.1016/j.agrformet.2014.03.016>
- LI-COR (2009). *LAI-2200 Plant canopy Analyser: Instruction Manual*, LI-COR Inc., Lincoln Nebraska, USA.
- Miller, J.B. (1967). A formula for average foliage density. *Australian Journal of Botany*, 15, 141-144.
- Moorthy, I., Miller, J R., Hu, B., Chen, J., & Li, Q. (2008). Retrieving crown leaf area index from an individual tree using ground-based lidar data. *Canadian Journal of Remote Sensing*, 34(3), 320-332. doi: 10.5589/m08-027
- Morisette, J.T., Baret, F., Privette, J.L., Myneni, R.B., Nickeson, J., Garrigues, S., et al. (2006). Validation of global moderate-resolution LAI Products: a framework proposed within the CEOS Land Product Validation subgroup, *IEEE Transactions on Geoscience and Remote Sensing*, 44 (7) p.1804 - 1817.
- Neumann, H.H., Den Hartog, G., Shaw, R.H., 1989. Leaf area measurements based on hemispheric photographs and leaf-litter collection in a deciduous forest during autumn leaf-fall. *Agricultural and Forest Meteorology*. 45, 325-245.
- Newnham, G., Armston, J., Muir, J., Goodwin, N., Tindall, D., Culvenor, D., Püschel, P., Nyström, M., & Johansen, K. (2012). Evaluation of Terrestrial Laser Scanners for Measuring Vegetation Structure. In C. S. A. Flagship (Ed.): CSIRO.
- Norman, J.M. & Campbell, G.S. (1989). *Plant Physiological Ecology: Field Methods and Instrumentation*. Eds., Pearcy, R.W., Ehleringer, J.R., Mooney, H.A. & Rundel, P.W. (London: Chapman and Hall) p. 301-325.
- Pisek, J., Lang, M., Nilson, T., Korhonen, L., & Karu, H. (2011). Comparison of methods for measuring gap size distribution and canopy nonrandomness at Järvelja RAMI (RAAdiation transfer Model Intercomparison) test sites. *Agricultural and Forest Meteorology*, 151(3), 365-377. doi: <http://dx.doi.org/10.1016/j.agrformet.2010.11.009>
- Prince, S.D. (1991) A model of regional primary production for use with coarse resolution satellite data. *International Journal of Remote Sensing* 12 (6) 1313-1330.
- Raumonen, P., Kaasalainen, M., Åkerblom, M., Kaasalainen, S., Kaartinen, H., Vastaranta, M., Holopainen, M., Disney, M., & Lewis, P. (2013). Fast automatic precision tree models from terrestrial laser scanner data. *Remote Sensing*, 5(2), 491-520.
- Ross, J. (1981) The radiation regime and architecture of plant stands. *Dr. W. Junk Publishers*, The Hague, Netherlands. pp 392.

Ryu, Y., Nilson, T., Kobayashi, H., Sonnentag, O., Law, B.E. & Baldocchi, D.D. (2010). On the correct estimation of effective leaf area index: Does it reveal information on clumping effects? *Agricultural and Forest Meteorology*, 150 (3) p. 463 - 472.

Sea, WB, P Choler, J Beringer, RA Weinmann, LB Hutley and R Leuning (2011). Documenting improvement in leaf area index estimates from MODIS using hemispherical photos for Australian savannas. *Agricultural and Forest Meteorology* 151: 1453–1461.

Strahler, A. H., Jupp, D. L. B., Woodcock, C. E., Schaaf, C. B., Yau, T., Zhau, F., Yang, X., Lovell, J., Culvenor, D., Newnham, G., Ni-Meister, W. and Boykin-Morris, W. (2008) Retrieval of forest structural parameters using a ground-based lidar instrument (Echidna®). *Canadian Journal of Remote Sensing* **34** (2) S426-S440.

Tian, Y., Woodcock, C.E., Wang, Y., Privette, J.L., Shabanov, N.V, Zhou, L. et al. (2002). Multiscale analysis and validation of the MODIS LAI product I. Uncertainty assessment, *Remote Sensing of Environment*, 83 p. 414 - 430.

Weiss, M., Baret, F., Garrigues, S. and Lacaze, R. (2007) LAI and fAPAR CYCLOPES global products derived from VEGETATION. Part 2: validation and comparison with MODIS collection 4 products. *Remote Sensing of Environment* **110** 317-331.

Weiss, M. and Faret, F. (2010). CAN-EYE v6.1 User Manual. French National Institute of Agronomical Research (INRA). <https://www4.paca.inra.fr/can-eye>

Weiss, M. and Baret, F. (2011). fAPAR (fraction of Absorbed Photosynthetically Active Radiation) estimates at various scale. *34<sup>th</sup> International Symposium on Remote Sensing of Environment*.

White, M.A., Asher, G.P., Neman, R.R., Privette, J.L. & Running, S.W. (2000). Measuring Fractional cover and Leaf Area Index in Arid Ecosystems: Digital Camera, Radiation Transmittance and Laser Altimetry Methods, *Remote Sensing of Environment*, 74 p. 45 – 57

Whitford, K.R., Colquhoun, I.J., Lang, A.R.G. & Harper B.M. (1995). Measuring leaf area index in a sparse eucalypt forest: a comparison of estimates from direct measurement, hemispherical photography, sunlight transmittance and allometric regression, *Agricultural and Forest Meteorology*, 74 p. 237 - 249.

Wilson, J. (1963). Estimation of foliage denseness and foliage angle by inclined point quadrats. *Australian Journal of Botany*, 11(1), 95-105. doi: <http://dx.doi.org/10.1071/BT9630095>

Woodgate, W., Disney, M., Armston, J.D., Jones, S.D., Suarez, L., Hill, M.J., Wilkes, P., Soto-Berelov, M., Haywood, A., & Mellor, A. (in review). Quantifying the impact of ignoring woody material in estimating canopy gap fraction and Leaf Area Index in woody ecosystems. *Remote Sensing of Environment*.

Woodgate, W., Jones, S.D., Suarez, L., Hill, M.J., Armston, J.D., Wilkes, P., Soto-Berelov, M., Haywood, A., & Mellor, A. (In review). Understanding the variability in ground-based methods for retrieving Canopy Openness, Gap Fraction, and Leaf Area Index in diverse forest systems. *Agricultural and Forest Meteorology*.

Zheng, G. & Moskal, L.M. (2009). Retrieving Leaf Area Index (LAI) Using Remote Sensing: Theories, Methods and Sensors, *Sensors*, 9, p. 2719 - 2745.

## Websites

---

### WWW1

<http://lpvs.gsfc.nasa.gov>

### WWW2 (TLSIIG)

[http://128.197.168.195/?page\\_id=37](http://128.197.168.195/?page_id=37)

or

TLIIIG. (2014). Terrestrial Laser Scanning International Interest Group. Retrieved 21/02/2014, from [http://128.197.168.195/?page\\_id=37](http://128.197.168.195/?page_id=37)

#### **WWW3**

[http://daac.ornl.gov/BIGFOOT\\_VAL/bigfoot.shtml](http://daac.ornl.gov/BIGFOOT_VAL/bigfoot.shtml)

#### **WWW4**

<http://data.auscover.org.au/xwiki/bin/view/Field+Sites/Star+Transect+Protocol+Web+Page>

#### **WWW5**

<http://www.tern.org.au/AusPlots-Rangelands-pg17871.html>

#### **WWW6**

[http://data.auscover.org.au/xwiki/bin/view/Field+Sites/Hemispheric\\_Protocol](http://data.auscover.org.au/xwiki/bin/view/Field+Sites/Hemispheric_Protocol)

#### **WWW7**

<http://data.auscover.org.au/xwiki/bin/view/Field+Sites/LAI2200+Protocol>

#### **WWW8**

[http://thredds0.nci.org.au/thredds/catalog/u39/modis/lpdaac-mosaics-cmar/v1-hdf4/aust/MOD15A2.005/catalog.html?dataset=u39/modis/lpdaac-mosaics-cmar/v1-hdf4/aust/MOD15A2.005/MOD15A2.005\\_2012.tar](http://thredds0.nci.org.au/thredds/catalog/u39/modis/lpdaac-mosaics-cmar/v1-hdf4/aust/MOD15A2.005/catalog.html?dataset=u39/modis/lpdaac-mosaics-cmar/v1-hdf4/aust/MOD15A2.005/MOD15A2.005_2012.tar)

## **Appendix A**

---

The CEOS WGCV LPV Subgroup has just published a Good Practice Protocol for the validation of LAI Products. The document is available for download here, as are other supporting documents:

[http://lpvs.gsfc.nasa.gov/LAI\\_background.html](http://lpvs.gsfc.nasa.gov/LAI_background.html)

## **Acronyms**

---

ALS – Airborne laser scanning

CEOS – Committee on earth observation satellites

CSIRO – Commonwealth scientific and industrial research organisation

DHP – Digital hemispherical photography

ECV – Essential climate variable

FAPAR,  $f_{\text{APAR}}$  – Fraction of absorbed photosynthetic active radiation

FCOVER – Vegetation cover fraction

GPS – Global positioning system

LAI – Leaf area index

LAI<sub>e</sub> – Effective leaf area index

LPV – Land product validation

PAI – Plant area index

PAI<sub>e</sub> – Effective plant area index

PAR – Photosynthetic active radiation

SAI – Surface area index

SLA – Specific leaf area

TERN – Terrestrial ecosystem research network

TLS – Terrestrial laser scanning

WGCV – Working group on calibration and validation